Wind pattern clustering of high frequent field measurements for dynamic wind farm flow control

Becker, M.; Allaerts, D.J.N.; van Wingerden, J.W.

DOI
10.1088/1742-6596/2767/3/032028

Publication date
2024

Document Version
Final published version

Published in
Journal of Physics: Conference Series

Wind pattern clustering of high frequent field measurements for dynamic wind farm flow control

Journal of Physics: Conference Series **2767** (2024) 032028 doi:10.1088/1742-6596/2767/3/032028

Wind pattern clustering of high frequent field measurements for dynamic wind farm flow control

M Becker[1], D Allaerts[2], J W van Wingerden[1]

[1] Delft Center for Systems and Control, Delft University of Technology, Mekelweg 2, 2628 CD Delft, NL

[2] Faculty of Aerospace Engineering, Delft University of Technology, Kluyverweg 1, 2629 HS Delft, NL

E-mail: marcus.becker@tudelft.nl

Abstract. In this work, we investigate a method to derive characteristic dynamic flow field behavior from field measurements. We further explore how these changes impact the performance of a wind farm flow control strategy. For a long time, hourly to 10-min averaged data has been the predominant form to store meteorological quantities such as wind speeds and wind directions. With the decreasing cost of digital storage and improvements in measurement technology, the assimilation of higher frequent data has become more feasible. We use one of these open-source datasets provided by the KNMI to explore what characteristic flow behavior is described in the high-frequency recordings of a Wind-LiDAR located in the North-Sea. To this end we employ a K-Means algorithm to cluster 10-min time series of wind direction changes sampled at 20 s. Our study finds that the majority of wind direction changes within this time window can be described by five main clusters with clock- and counterclockwise changes of the wind direction in the range of ± 4 deg. Subsequently we investigate the implications for quasi-steady wind farm flow control. We employ look-up table yaw-steering control next to baseline control in selected cases in a turbulent Large Eddy Simulation to verify the predictions made by a dynamic parametric engineering wake model. We find good agreement between both simulation environments and use the engineering model to investigate all wind directions in 2 deg resolution. The results show that the identified wind direction changes can have a significant negative impact on the power generated by a 10 turbine wind farm. The study also shows that the fixed yaw-steering set-points are still favorable over baseline operation for wind direction changes in the range of ± 1.6 deg, but can act detrimental for larger changes.

1. Introduction

Wake steering is one method of wind farm flow control (WFFC). It utilizes the fact that a wind turbine's misalignment with the main wind direction will lead to a deflected wake. This can be used to "steer" the turbine's wake away from a downstream turbine. The upstream turbine experiences a power loss, but the power generated by the downstream turbine can be significantly increased [1].

How to set the yaw angle of a turbine depends on the wind farm layout and the flow conditions. The latter encapsulates wind speed, direction and atmospheric stability. One existing approach to apply wake steering is to offline generate yaw angle look-up-tables (LUT) for various flow conditions [2]. During operation, the controller identifies the current flow conditions and applies the previously derived setpoints. The complexity of these LUT depends on the flow conditions

considered. In their simplest form, these are composed of a discrete range of relevant wind speed and wind direction bins. To find accurate setpoints for each combination, fast-running engineering models have been derived (e.g. [3]). These approximate the wind farm flow field at a low computational cost and estimate how the farm power will be affected by a given yaw angle choice. An optimization algorithm is then used to determine the ideal yaw angle for each turbine. Most of these engineering models rely on steady state assumptions, and aim to predict the mean wind farm flow field given a constant wind direction and speed. This, in return, limits a derived LUT approach, which can only act based on the results derived in steady-state.

The question arises to which extend the steady-state assumption limits the yaw-steering control approach. Formulated in a different way, how does a steady-state controller perform once this assumption is violated?
To approach this question, a deeper understanding of the governing flow field behavior is required. To this end, historical data can be used to identify reoccurring flow characteristics. One approach to identify local wind patterns is presented by [4]. It uses one year of 10-minute averaged data, split into sequences that describe one day. Similar days are then fused and form a group. The study arrives at 31 centroids assembled in a decision tree, where similar centroids are close to one another. In [5] they describe an approach to cluster hourly resolved atmospheric data across the UK. The work results in an improved approach to 1- to 6-hour-ahead forecasts. To achieve this, atmospheric patterns are found by k-means clustering, followed by a self-organizing map. The latter describes a 2-layer artificial neural network that sorts a given set of input vectors. A probabilistic decision tree approach is presented by [6]. It categorizes wind farm power generation based on factors such as hourly to annual wind speed, farm area, and capacity factor. The study applies a K-Means clustering to the data before sorting the centroids into a Naïve Bayes tree. Similarly, [7] utilizes wind pattern clustering of hourly data in direct connection to turbine power to derive a wind farm power forecast model.

As indicated by the literature, it is possible to determine characteristic flow field patterns by clustering historical datasets. However, the considered low temporal resolution could hide flow dynamics relevant to turbine-to-turbine interactions and therefore important to WFFC strategies. Higher-frequent measurement datasets like [8] allow us to consider the transients within a 10-minute average data bin. Once decomposed into characteristic trajectories, these datasets can serve as a basis to study the effect of flow changes on the wind farm performance. They further give an insight into the magnitude and frequency at which the steady-state assumption is violated.

The main contribution of this work is twofold: (i) we provide a versatile data-driven method to extend the steady-state assumption of the wind rose and to incorporate dynamics, (ii) we utilize this tool to evaluate the impact of identified characteristic flow field behavior on the perfromance of wind farm flow control algorithms. In addition, the results of this work show how high frequent data can be used to systematically evaluate wind farm flow control algorithms and how it could be used to lead to more robust control actions.

The remainder of this paper is structured as follows: Section 2 introduces the methods used to prepare the flow field dataset, to cluster the data and to apply wind farm flow control techniques to it. Section 3 presents the results following the proposed methods. Section 4 concludes the work and points into possible directions of future work.

2. Methodology

2.1. Data preparation

The flow-field data is recorded by a ZephIR 300M wind lidar at the Borssele Alpha TenneT Platform in the North Sea between November 2019 and July 2023 [8]. Among other data it provides measurements of the horizontal and vertical wind speed, as well as the wind direction at eleven heights from 14 m to 249 m. In this work we exclusively use the horizontal wind speed

and wind direction at 119 m. This is equal to the hub height of the DTU 10 MW reference turbine [9], which we will use for the wind farm simulations. The data is segmented into time sections with sufficient completeness, and then interpolated using cubic splines from an irregular 1/17 to 1/22 Hz sampling frequency to consistent 1/20 Hz. The signal is filtered with a zero-phase Butterworth filter with a cut-off frequency of 1/400 Hz. The resulting data segments are assembled as 30 time step long "trajectories" or time series. Since the used dataset is recorded within an operational wind farm, we have to assume that the wind speed is strongly influenced by the wind turbines surrounding the measurement location. The wind speed data is therefore disregarded for this study, and only the wind direction information is kept.

2.2. Wind pattern clustering

To determine underlying patterns of the flow field the trajectories are combined in clusters. The assumption is that the cluster centroid is representative for the behavior of all trajectories combined in its cluster. We are employing a hard K-means clustering algorithm to derive these centroids [10]. This choice is in line with the previously discussed work on wind pattern clustering. To combat the impact of increased turbulence levels due to the measurement location within a wind farm, a large number of trajectories is combined in each centroid. The wind direction fluctuations will still appear in the data as variance of the centroid, but the mean behavior provides a low-pass filtered view on the underlying wind direction changes. As we are interested in the wind direction changes, we further calculate the difference of the wind direction values in the trajectory to its starting wind direction. As a result, all trajectories start at $\Delta\varphi = 0\,\mathrm{deg}$ before they diverge. To investigate for which wind directions the found difference-trajectories are valid, we bin all trajectories by their initial wind direction. Since there is a centroid for every trajectory, we can determine if a centroid is representative for all initial wind directions or only for a subset.

The hard K-means algorithm is based on the Euclidean distance:

$$d(\mathbf{t}_1, \mathbf{t}_2) = \|\mathbf{t}_2 - \mathbf{t}_1\|_R\,, \tag{1}$$

where $\|\cdot\|_R$ indicates that the calculation corrects for the radial nature of the dimensions. In a first step, the distance of each trajectory and a prescribed number of centroids is calculated and each trajectory is assigned to the closest centroid. In the second step, each centroid changes its position to the mean coordinates/values of the trajectories assigned to it. Both steps are repeated until either the position of the centroids is converged, or a maximum number of iterations is reached. The term "hard" refers to the fact that each trajectory belongs to one centroid.

2.3. Wind farm simulation

A subset of ten turbines of the Hollandse Kust Noord (HKN) wind farm is used to determine the impact of the wind direction changes. As there is no publicly available turbine model of the installed 11 MW turbines, we use the 10 MW DTU reference turbine [9]. The turbine locations are re-scaled such that the distance between the turbine is equivalent by turbine diameters (D) to the original layout. The selected turbines form the south-west corner of the wind farm. This layout has also been used in [11] and offers various turbine-to-turbine interactions: There are closely spaced turbines at ≈ 5 D, as well as wake interactions with a distance of > 20 D.

Three models are used to simulate the wind farm: the two engineering models FLORIS and FLORIDyn, as well as the LES wind farm model SOWFA:

The FLOw Redirection and Induction in Steady State (FLORIS) model is used to derive a naive lookup-table (LUT) controller using yaw steering [3]. To this end, the serial refine method [12] is used to determine the optimal yaw angles for the turbines to maximize the power generated based on the current wind direction. Following [2] we assume a dead-band controller that only

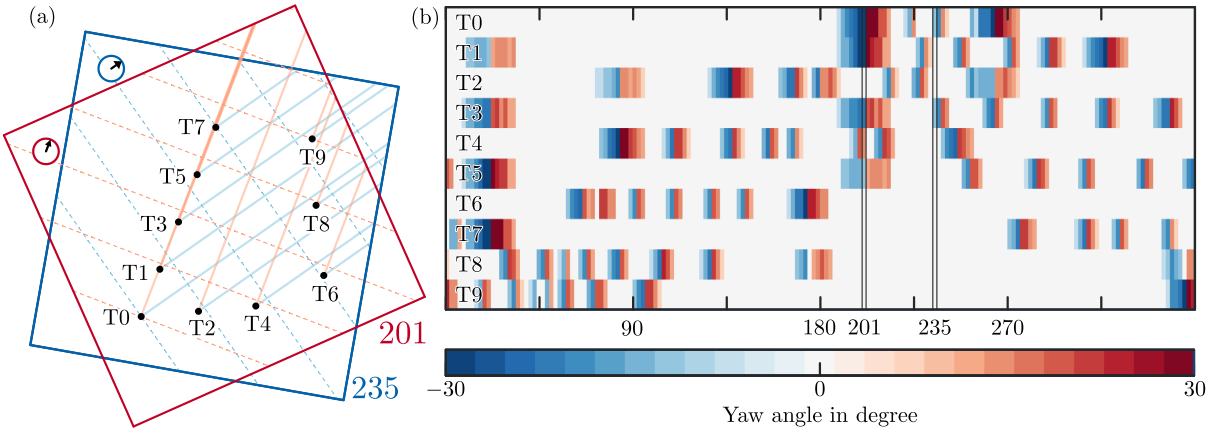

Figure 1. (a) HKN south-west corner wind farm layout with the domain rotated to fit the initial wind direction of 235 deg and 201 deg. The dotted cross-stream lines indicate the downstream distance of the turbines with respect to the most upstream turbine in 5 D steps. The downstream lines indicate along which line the wakes of the turbines are expected to develop. Subplot (b) depicts the steady-state yaw angle control policy derived using FLORIS.

updates the yaw set-points once the mean wind direction exceeds a set difference to the previous wind direction. The baseline controller acts identical, but always prescribes a yaw misalignment angle of 0 deg once the wind direction is updated. In this study we assume the dead-band to be ±5 deg. From the available wake models in the FLORIS toolbox, we employ the cumulative curl model [13].

The FLOw Redirection and Induction Dynamics (FLORIDyn) model is a dynamic version of FLORIS [14]. It models the wake behavior due to turbine state changes and flow changes based on Lagrangian particles that propagate downstream with the flow. This implementation of FLORIDyn interfaces directly with the FLORIS code and offers equal results in steady state conditions, enhanced by flow dynamics. We use this model to approximate the impact of the wind direction changes onto the power generated by the wind farm. To this end we choose 180 starting wind directions: from 1 deg to 359 deg in 2 deg steps. The turbine orientations are initialized based on the LUT value for the initial wind direction. After a transient period of 700 s for the wakes to develop, the 600 s wind direction change takes place, prescribed by a centroid deducted from the measurement data (see Section 2.2). The transition is followed by another 700 s transient period for the wakes to settle in the new wind direction. The simulation time totals to 2000 s, resolved in 4 s steps. All 180 wind directions are simulated twice for every selected centroid, once with a yaw steering controller, once with no yaw misalignment with the initial wind direction. The low computational cost of FLORIDyn does allow us to simulate the large quantity of dynamic simulations[1].

The Simulator for Offshore Wind Farm Applications (SOWFA) is used to verify the results given by FLORIDyn [15]. The turbines are modeled as Actuator Discs (ADM) in a $5 \times 5 \times 1$ km domain in a neutral atmospheric boundary layer, discretized into $20 \times 20 \times 10$ m cells. To drive the simulation, a single precursor is generated over 30000 s with a main wind direction of 225 deg. It is followed by successor simulations of 2000 s during which the wind direction uniformly changes based on the selected centroid data. The free wind speed forced at hub height (119 m) is 9 ms^{-1}, with a turbulence intensity of 5.4%. Figure 2 depicts the shear and veer profile of the LES simulation. The precursor is run with a 1 s time step, the wind farm

[1] Code and example cases are available at https://doi.org/10.4121/dbd831b5-8d6d-4ae2-9860-2d6a7a1be58e

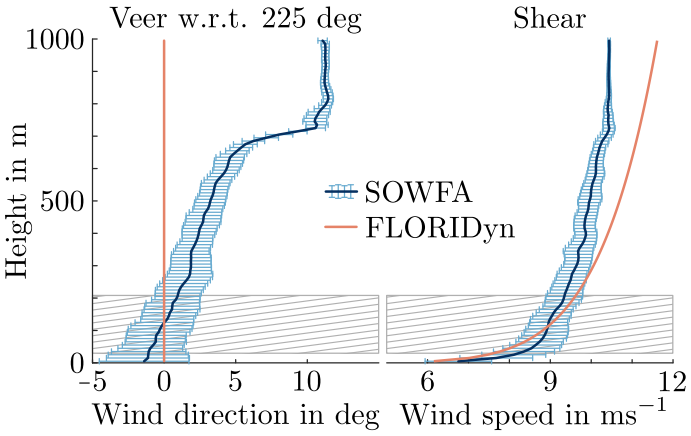

Figure 2. Veer and shear profile of the precursor used in the SOWFA simulations. The orange line depicts the settings used for the FLORIDyn simulations. The grey, striped area indicates the rotor swept area. The LES measurements are given with one standard deviation.

simulation with a 0.5 s time step. To simulate the wind farm in different main wind directions, the wind farm is rotated rather than the main wind direction, see Figure 1 (a).

3. Results

3.1. Wind pattern clustering

The K-means algorithm described in Section 2.2 was tested with $K \in [1, 360]$. A suitable trade-off between within-cluster-error and number of clusters was found for $K = 15$. Multiple randomly initialised starts indicated that the majority of the trajectories is predominately captured by 5 to 7 symmetrical clusters. Figure 3 (a) depicts the five dominant wind direction clusters chosen for this study. They cumulatively represent 87% of the data set. Each cluster contains between 18.6k and 36.4k members. The clusters can be split into one steady wind direction time series, two increasing and two decreasing ones. For each change the clustering finds one strong change of approximate 4 deg and a moderate one of 1.6 deg. The clusters cover 80 to 90% of the time series in most 5 deg wind direction bins, as can be seen in Figure 3 (b). An exception is the area between 300 and 330 deg, which suggests that the time series found there are more extreme than the dominant ones[2]. The question arises how these wind direction changes have an affect on the performance of a wind farm and the control strategy that is being applied. Section 3.2 further investigates this question.

3.2. Wind farm simulation

3.2.1. The impact of wind direction changes starting at 201 deg and 235 deg At 201 deg wind direction, the turbines T0, T1, T3, T5 and T7 stand in line, with approximately 4 D spacing, see Figure1. In addition, T4 wakes T9 over a distance of 15 D. This scenario features multiple wakes overlapping and very few turbines that are unwaked. WFFC strategies have thereby the potential to significantly improve the farm power generation. At 235 deg wind direction, far-wake interactions dominate: T0 wakes T8 with roughly 18 D spacing, T3 wakes T9 with 15 D spacing. Given the spacing we expect significant delays between the turbines, but we also expect a near 100% power generation of the wind farm, as only far wake effects are present. The cases will be denoted by *C•-201deg-∘*, where • denotes the wind direction time series 1 to 5, see Figure 3, and ∘ is either replaced by *BL* for Baseline or *Yaw* for the respective control strategy.

During the comparison of the SOWFA and FLORIDyn cases it became clear that there is a significant mismatch in absolute power generated by the wind farm: In C3-235deg-BL, the SOWFA wind farm generates an average of 70.42 ± 1.78 MW, as opposed to FLORIDyn with

[2] The data and the code to produce these results is available at https://doi.org/10.4121/02cbb452-4900-4c0a-95ae-5bdb5ce42ed7

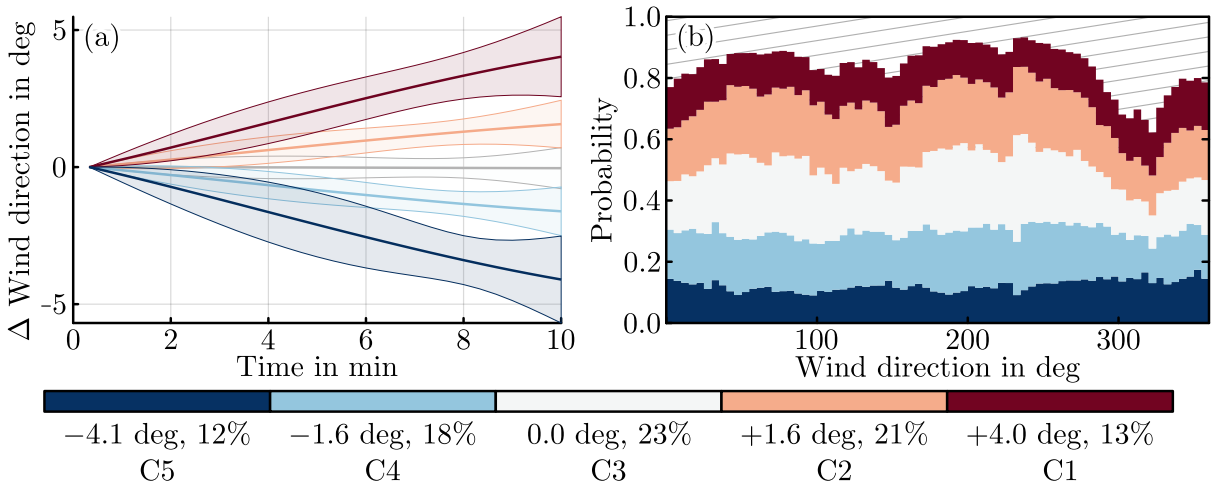

Figure 3. (a) Wind direction centroids with one standard deviation, (b) as well as their distribution across all wind directions.

50.53 MW. Similarly SOWFA generates an averaged of 50.92 ± 7.19 MW in C3-201deg-BL, and FLORIDyn 35.09 MW. Looking at C3-235deg-BL, we would expect the wind farm to operate at almost 100% as only T8 and T9 are waked over a far distance. Given a free wind speed of 9ms^{-1} and the power curve of the turbine [9] we would expect a power generation of roughly 50 MW for a 10 turbine wind farm. This is reflected by FLORIDyn, but not by SOWFA. We attribute the overestimation of the power generated in SOWFA by the way the effective wind speed is sampled by the ADM on the coarse LES grid [16]. Given the cubed relation between generated power and wind speed $P \propto u^3$, an overestimation of the wind speed leads to a much larger overestimated power. For the remainder of the paper we will therefore rely on the normalized power to detect trends and relations between the simulation environments and compare those.

Figure 4 (a & b) show the power generation ratio of LUT control to baseline control as predicted by FLORIDyn and as simulated by SOWFA. Figure 4 (a) depicts the wind farm power as the flow field is subject to the wind direction changes C1 and C5, starting from 201 deg (see Figure 3). During the initialization, FLORIDyn shows how the effect of the LUT yaw angles propagating through the wind farm: A significant initial loss due to yaw misalignment is recouped by a step-wise increase of the turbine performance as a result of the favorable wake positions. This leads to a predicted power generation improvement of $\approx 10\%$. The wind direction change happens between $t = 700$ s and 1300 s, which initiates the divergence of the trajectories. Starting with the wind direction change, we see that the performance of the wind farm significantly deteriorates in the C1 case in comparison to the previous performance and the baseline performance. This is explained by the fact that the wind direction change forces a strong wake overlap in the wind farm which the LUT initially tried to prevent. As a result, the wakes are steered into the turbines instead of away from them. This is also reflected in the LUT, see Figure 1 (b) where the yaw angle setpoints switch from large negative values to large positive ones for T0, T1, T3 and T5.

Figure 4 (b) compliments the results of (a) with the wind direction change starting at 235 deg instead. The initial underperformance of the wind farm is now prolonged as the turbines that benefit from the wake redirection are located 15 to 18 D downstream of the misaligned turbines. C1 changes the wind direction from 235 deg to 239 deg, which initially leads to a decrease of the yaw misalignment of the turbines T0 and T3 and therefore to a higher power generation overall. However, the new wind direction also leads to a unfavorable stronger waking

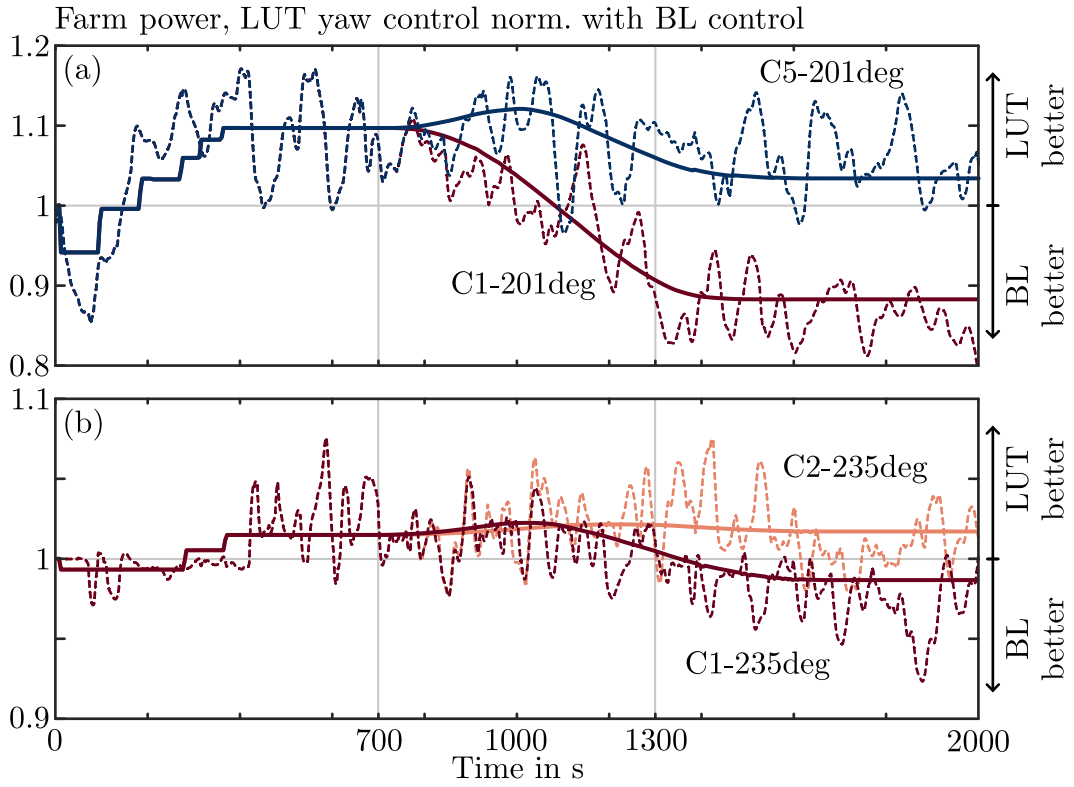

Figure 4. Power generation of the wind farm starting from (a) 201 deg initial wind direction, and (b) 235 deg. The power generated is normalised by the wind farm with the same wind direction change using baseline control. The dotted lines are the SOWFA time series, the continuous lines from FLORIDyn. The mean wind speed is constant during the simulations.

of T6, T8 and T9 which causes a delayed decrease in wind farm performance. This leads to a sub-optimal performance of the LUT controller in comparison to the baseline controller. In both cases, Figure 4 (a) and (b) we see that a wind direction change does not necessarily lead to a decreased performance of the controller. In the C2-235deg case for instance, the LUT approach remains the better choice in comparison to the baseline performance. This is also true for the larger direction change in the C5-201deg case.

Figure 5 depicts the farm energy, integrated starting at $t = 600$ s, to judge if and how much the wind farm performance has suffered due to the wind direction change. The plot indicates that the gain achieved by wake steering persists throughout four of the five cases. In the C5 case however, the performance is detrimental, which is in line with Figure 4 (a).

Comparing FLORIDyn and SOWFA overall, we can see a qualitative agreement between the trends of the two simulators. While FLORIDyn cannot predict the turbulent fluctuations of the LES simulation, it does predict the overall trend of the validation simulations and how one control strategy compares to the other. In the farm energy cases (see Figure 5) FLORIDyn consistently overpredicts the farm performance by one to two percent points. The curves also show a converging relation, which points to an overall good agreement between the simulations. The nature of the turbulent simulations makes it difficult to identify more nuanced differences between SOWFA and FLORIDyn. Rerunning and averaging the LES simulations multiple times with different turbulence generations could indicate where FLORIDyn might lack wake dynamics relevant to a WFFC application. A longer time series would also indicate how the performance

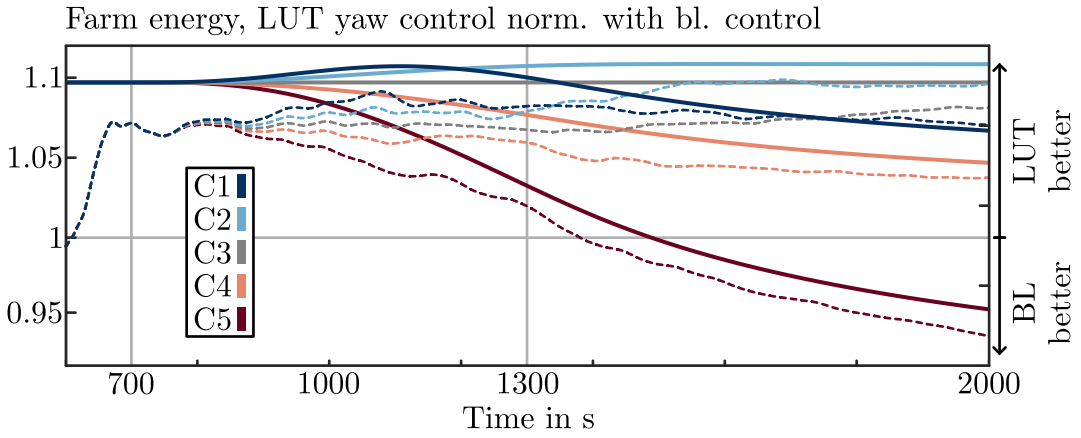

Figure 5. Normalised energy generation derived from the integral of the farm power starting at t= 600 s from the initial wind direction of 201 deg. The dotted lines are the SOWFA time series, the continuous lines from FLORIDyn.

compares on a continuous basis. For this work we conclude that FLORIDyn is sufficiently accurate to predict the dynamic trends of yaw-based wind farm flow control strategies.

3.2.2. Wind farm power across all wind directions Based on the results from Section 3.2.1 we broaden the range of investigated initial wind directions: Figure 6 depicts the farm performance for 180 initial wind directions from 1 deg to 359 deg in 2 deg steps. For each wind direction all clusters are simulated twice - once with the LUT approach and once with the baseline approach. This totals to 1800 simulations, or an aggregated 41.7 days of simulated wind farm behavior. Figure 6 (a) shows the raw data of the farm behavior starting at 235 deg over the simulation duration. After the ratio has converged, the power difference between the no-direction change case (C3) and the other cases is normalised by the performance of C3. As a result, we can see in Figure 6 (b) that the wind direction changes mainly lead to a worse performance for the LUT approach, compared to a steady wind direction. This aligns with the intuition that yaw steering would operate at a local optimum, and that a change of conditions has detrimental effects. Figure 6 (c) shows that baseline operation can benefit from wind direction changes. For most cases one wind direction change leads to an improvement while the opposite direction has a negative influence - in one case the wake overlap is decreased, in the other one it is increased. The performance of both is compared in Figure 6 (d), red indicates a superior performance of the LUT approach, while a better performance of the baseline is indicated by a blue color. The figure shows that yaw steering is consistently a better choice for small wind direction changes, but underperforms for wind direction larger wind direction changes of ±4 deg.

Figure 6(e-f) depict the same content as Figure 6(b-d) but for the energy generated. The interpretation remains largely the same, only Figure 6(f) indicates that the initial gain due to yaw-steering might not be entirely lost at the end of the simulation.

4. Conclusion

In this work we showcase a method to compress high frequent wind direction change time series into a small number of representative clusters. This makes wind directions changes tangible and provides a test bench for wind farm flow control approaches. As a demonstration we applied the five most dominant cluster time series to two basic farm controllers: a baseline controller with the turbines aligned with the initial wind direction and a lookup table yaw steering controller. Both

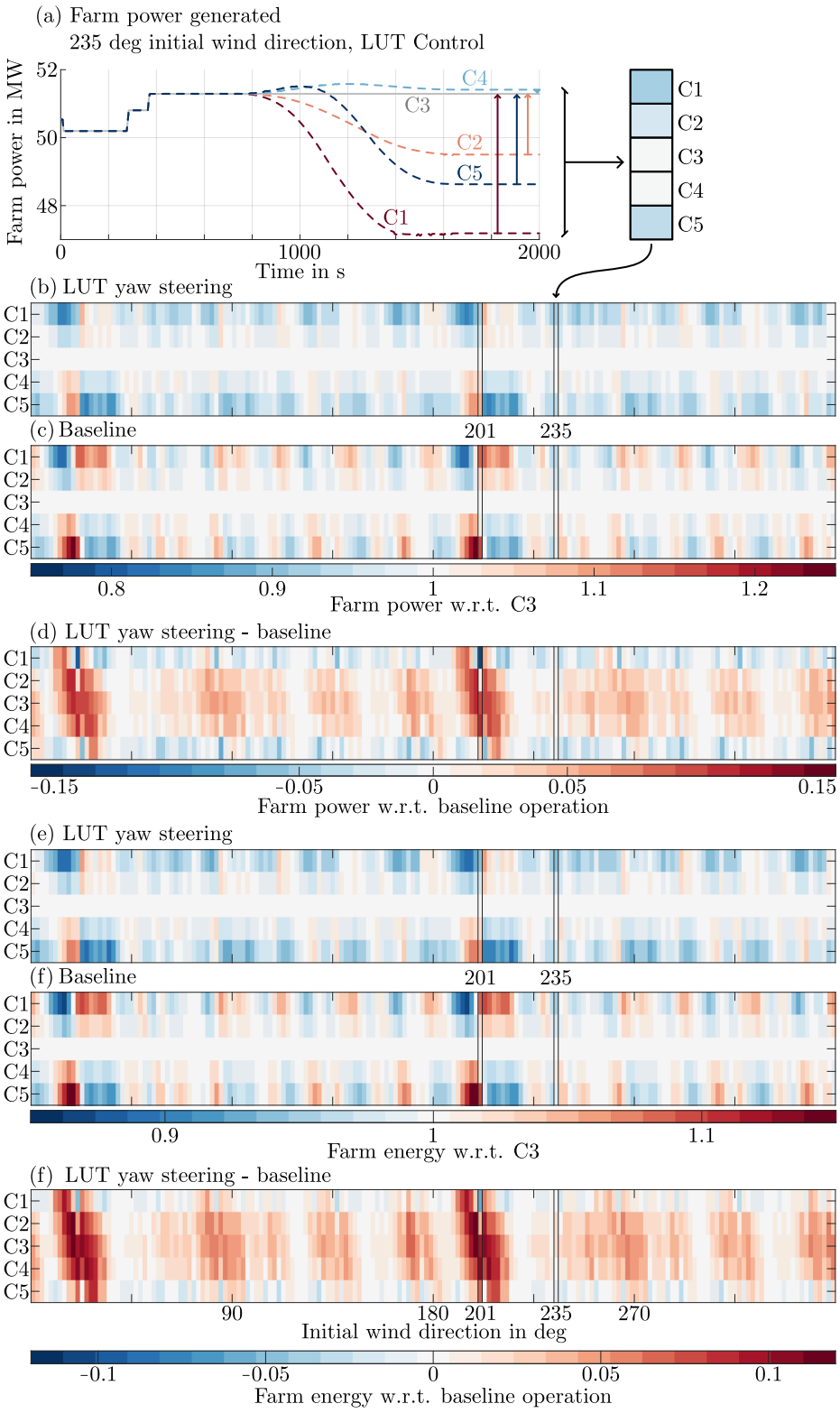

Figure 6. Normalised power (b-d) and energy (e-f) generated by the wind farm for five wind direction time series and 180 initial wind directions with $u_\infty = 9\text{ms}^{-1}$. Subplot (a) depicts how the values for (b-d) are derived, (e-f) are based on the integral from $t = 700$ s to 2000 s.

controllers were tested in ten scenarios in the LES code SOWFA and the dynamic engineering model FLORIDyn. Two central takeaways from the study are that 1) wind direction changes in the range of $[-4.1, 4]$ deg can have a significant impact on the power generated by the wind farm and 2) that the FLORIDyn prediction of the farm's power is sufficiently accurate to derive trends between controllers that are in line with the reference LES behavior. Based on this a broader study with 180 initial wind directions was conducted that reveals that the tested wake steering controller yields a consistent performance improvement for small wind direction changes, but can lead to detrimental performance for larger changes.

For future work we recommend considering a larger dataset, and to correct for other factors such as wind speed regimes, atmospheric stability, time of day and seasons. This work could further lead to a dynamic approach to estimate the annual-energy-produced and to systematically investigate the impact of the used control strategy onto the structural loads in the presence of changing flow. Lastly, this approach could be used to aid a robust optimization of real-time wind farm flow control strategies by providing different scenarios as well as their likelihood.

Acknowledgement This work is part of the research programme Robust closed-loop wake steering for large densely space wind farms with project number 17512 and partly financed by the Dutch Research Council (NWO).

References

[1] J. Meyers, C. Bottasso, K. Dykes, P. Fleming, P. Gebraad, G. Giebel, T. Göçmen, and J.W. Van Wingerden. Wind farm flow control: Prospects and challenges. *Wind Energy Science*, 7(6):2271–2306, November 2022.
[2] S. Kanev. Dynamic wake steering and its impact on wind farm power production and yaw actuator duty. *Renewable Energy*, 146:9–15, February 2020.
[3] NREL. FLORIS. Version 3.4. *GitHub repository*, November 2023.
[4] V.M. Gómez-Muñoz and M.A. Porta-Gándara. Local wind patterns for modeling renewable energy systems by means of cluster analysis techniques. *Renewable Energy*, 25(2):171–182, February 2002.
[5] J. Browell, D. R. Drew, and K. Philippopoulos. Improved very short-term spatio-temporal wind forecasting using atmospheric regimes: Improved very short-term spatio-temporal wind forecasting using atmospheric regimes. *Wind Energy*, 21(11):968–979, November 2018.
[6] M. Khan, C. He, T. Liu, and F. Ullah. A New Hybrid Approach of Clustering Based Probabilistic Decision Tree to Forecast Wind Power on Large Scales. *Journal of Electrical Engineering & Technology*, 16(2):697–710, March 2021.
[7] N. Goudarzi and D. Ziaei. Wind Farm Clustering Methods for Power Forecasting. In *ASME 2022 Power Conference*, page V001T07A015, Pittsburgh, Pennsylvania, USA, July 2022. American Society of Mechanical Engineers.
[8] S. Knoop. Wind - lidar wind profiles measured at North Sea wind farm TenneT platforms 1 second raw data, November 2019.
[9] C. Bak, F. Zahle, R. Bitsche, T. Kim, A. Yde, L. Christian Henriksen, M. H. Hansen, J. P. A. A. Blasques, M. Gaunaa, and A. Natarajan. The DTU 10-MW Reference Wind Turbine. May 2013.
[10] H. Steinhaus. Sur la division des corps matériels en parties. *Bulletin de l'académie polonaise des sciences*, 4(12):801–804, October 1956.
[11] M. J. Van Den Broek, M. Becker, B. Sanderse, and J. W. Van Wingerden. Dynamic wind farm flow control using free-vortex wake models. *Wind Energ. Sci. Discuss. [preprint]*, September 2023.
[12] P. A. Fleming, A. P. J. Stanley, C. J. Bay, J. King, E. Simley, B. M. Doekemeijer, and R. Mudafort. Serial-Refine Method for Fast Wake-Steering Yaw Optimization. *Journal of Physics: Conference Series*, 2265(3):032109, May 2022.
[13] C. J. Bay, P. A. Fleming, B. M. Doekemeijer, J. King, M. Churchfield, and R. Mudafort. Addressing deep array effects and impacts to wake steering with the cumulative-curl wake model. *Wind Energy Science*, 8(3):401–419, March 2023.
[14] M. Becker, D. Allaerts, and J. W. van Wingerden. FLORIDyn - A dynamic and flexible framework for real-time wind farm control. *Journal of Physics: Conference Series*, 2265(3):032103, May 2022.
[15] NREL. Simulator for offshore wind farm applications. *GitHub repository*, November 2020.
[16] L. A. Martínez-Tossas, M. J. Churchfield, and S. Leonardi. Large eddy simulations of the flow past wind turbines: Actuator line and disk modeling. *Wind Energy*, 18(6):1047–1060, 2015.